IJPSR (2019), Volume 10, Issue 10 **(Research Article)**

INTERNATIONAL JOURNAL OF PHARMACEUTICAL SCIENCES AND RESEARCH

Received on 25 January 2019; received in revised form, 24 April 2019; accepted, 14 June 2019; published 01 October 2019

ASSESSMENT OF *IN-VITRO* ANTICANCER AND ANTIBACTERIAL ACTIVITIES OF *CARCHORUS HIRSUTUS* PHYTOMEDIATED OPTIMIZED NANOSILVER

Dongamanti Ashok [*1], Sandupatla Raju [2] and Koyyati Rama [2]

Green and Medicinal Chemistry Laboratory [1], Forensic Science Unit [2], Department of Chemistry, Osmania University, Hyderabad - 500007, Telangana, India.

Keywords:

Corchorus hirsutus, Nanosilver, Atomic force microscope, Anticancer, Antibacterial activities

Correspondence to Author:
Prof. Dongamanti Ashok

Green and Medicinal Chemistry Laboratory, Department of Chemistry, Osmania University, Hyderabad - 500007, Telangana, India.

E-mail: ashokdou@gmail.com

ABSTRACT: The elected work reports for the first time successfully synthesized nanosilver from the aqueous leaf extract of the *Carchorus hirsutus* plant. Because the phytochemicals within the leaf extract were creditworthy for the reduction of silver ions as the active nanosilver particles, in addition to this, they act as the capping agents who had been environed at the surface of the particles. UV-Vis spectroscopy oversaw the establishment of nanosilver as an appropriate peak detected at 412 nm of surface plasmon resonance has affirmed the colloidal nanosilver. The peaks of Fourier Transform Infrared Spectroscopy had proved to be phytochemicals responsible for the reduction of nanosilver. The crystalline structure and average diameter found to be 29 nm of the phytosynthesized nanosilver particles were found out using X-ray diffraction studies. The Scanning Electron Microscopy images were rendered the aggregated, semi-spherical to spherical silver nanocrystals. The elemental signals of energy dispersive X-ray spectrum substantiate the presence of silver detail as silver weight % is 86.84 and atomic % is 68.45. The atomic force microscope turned into used to take a look at the dimensions, topographical structure of the synthesized nanosilver. Then the antibacterial activity of synthesized nanosilver has been effectively examined by the well-diffusion method in opposition to four harmful bacteria *Staphylococcus aureus, Klebsiella pneumoniae, Pseudomonas putida,* and *Bacillus subtilis* as evincing high activity. The *Corchorus hirsutus* mediated nanosilver exerts their cytotoxic impact on MCF7 cell lines of breast adenocarcinoma cells and HeLa cell lines of cervical cancer cells.

INTRODUCTION: Present age nanotechnology is the trending research area. Around the globe, researchers from all fields of science and technology are researching nanoscience because of their huge range of applications.

QUICK RESPONSE CODE

DOI:
10.13040/IJPSR.0975-8232.10(10).4587-97

The article can be accessed online on
www.ijpsr.com

DOI link: http://dx.doi.org/10.13040/IJPSR.0975-8232.10(10).4587-97

The vast variety of novel programs were accomplished within the contemporary age of metallic nanoparticles that's why broader research has been continuing on this subject, and more has to be executed.

The epoch of nanotechnology and nano-associated discovering in the present has accelerated towards new technological developments and applications which imparts the interest in the commercial as well as the scientific community. The nanoparticles are dealing with the sizes below 100 nm ranges as the smallest particles; the activity was good due

increasing the surface area [1] while compared to the larger nanoparticles consequently the properties vary with the shape, surface structure, and distribution. Those all parameters are depending on discovering novel properties that have the outcome for use in various novel applications [2], so the nanotechnology is the coming forth discipline due to the fact it's miles anywhere in all areas of science and technology which include physics, chemistry, engineering, electronics, information technology, biochemistry, biotechnology, biomedical engineering, medicine, materials science, forensic science [3], textile, food technology [4], agriculture [5] and many more. In a maximum of the instances, the nanosilver particles constituted are highly unstable, so necessitate the addition of a separate capping agent which renders stability. It has been extensively stated that synthesis of nanosilver using plant extracts often leads to highly controlled size and morphology.

Moreover, such pathways are cost-effective, eco-friendly [6], use of poisonous chemical compounds, high pressure and temperatures are not required. The written reports unveiled that the nanosilver synthesized from sustainable or green chemistry methods possesses potent antibacterial properties [7, 8, 9, 10]. The establishment of plant-mediated metallic nanoparticles become a utilitarian area of research because the plants own the phytochemicals therein active compounds which were used to cure various diseases as they are medically essential. A wide range of literature available in the synthesis of nanoparticles from phytomediated called green chemistry strategies [11, 12, 13, 14], so the involvement of these phytochemicals from medicinal plants environed by means of nanoparticles, as a result, the combination of these active compounds with metallic nanoparticles evinced a wide range of revolutionary and advanced applications.

The picked out plant *Corchorus hirsutus* was used for the first time for the synthesis of nanosilver. Its common names are wooly booger and jackswitch belongs to the family Tiliaceae. The *Corchorus hirsutus* grows as a small to medium shrub up to 2m in height. The leaves are arranged alternately to 8 cm in length and 3 cm in width, ovate to oblong with a serrulate leaf margin and a rounded leaf apex. The *Corchorus hirsutus* leaves suitable for cooking and can be used for tea preparation. Jack-switch furnishes cowl for the natural world and enables guard the soil. The leaves have been used to treat colds and flu. The cutting-edge investigation stated toward the synthesis of surfactant-free metallic silver nanoparticles through the eco-friendly biological root using a medicinal plant *Carchorus hirsutus.* Therefore, the objectives of the comprehensive study are, to the synthesis of nanosilver particles using *Carchorus hirsutus* aqueous leaf extract act as reducing as well as a capping agent. To characterize the synthesized nanosilver and to evaluate the antibacterial property in opposition to four tested harmful microorganisms and assessment of *in-vitro* cytotoxic properties in opposition to MCF7, HeLa cell lines.

MATERIALS AND METHODS:

Materials: Fresh *Corchorus hirsutus* leaves had been picked up from the Osmania University Campus, Hyderabad, Telangana, India. Silver nitrate ($AgNO_3$) was purchased from S.D. Fine Chemicals and the chemicals utilized for antibacterial interest are of Himedia grade. The glassware utilized in the cutting-edge study was acid-washed very well and then rinsed with distilled water. DMEM (Dulbecco's modified Eagles medium), MTT [3-(4,5-dimethylthiazol-2-yl) -2,5-diphenyl tetrazolium bromide], trypsin, and EDTA Phosphate Buffered Saline (PBS) were purchased from Sigma Chemicals Co. (St. Louis, MO) and Fetal Bovine Serum (FBS) had been obtained from Gibco. 25 cm^2, 75 cm^2 flasks and 96 well plated bought from Eppendorf, India.

Preparation of *Corchorus hirsutus* Aqueous Leaf Extract: The *Corchorus hirsutus* leaves were thoroughly washed under running tap water initially to remove the cohered dirt particles present at the surface after which rinsed with distilled water. The **Fig. 1** of the elected plant leaves has been cleaned entirely after that dried at room temperature for 10 days.

The dried leaves were squashed into small pieces and stored in an airtight container at room temperature for further use. The selected mg of squashed leaves were mixed with 1000 ml of distilled water and kept for stirring at 60°C for 3 h, then the solution with phytochemicals withdrawn by means of filtering *via* Whatman no.1 filter paper

and the same was stored at 4°C. The clear leaf extract of *Corchorus hirsutus* thus received was used for the synthesis of nanosilver.

FIG. 1: THE *CORCHORUS HIRSUTUS* PLANT MATERIAL SELECTED FOR THE SYNTHESIS OF NANOSILVER

Optimized Synthesis of Nanosilver: Optimized synthesis and effect of parameters have been formerly reported [15, 16, 17]. To examine the impact of $AgNO_3$ concentration increased it by way of maintaining the plant extract concentration constant. Firstly, 5 mM of $AgNO_3$ stock solution was prepared afterward to make it into 1mM, 2mM, 3mM and 4mM as different concentrations in conical flasks and to that 10 ml of each solution, 10 ml of plant extract was added then observed at room temperature. Next, for the examination of the effect of the leaf extract concentration by way of maintaining the $AgNO_3$ concentration consistent.

The aqueous plant extract becomes prepared using dissolving 10 mg, 20 mg, 30 mg, 40 mg, 50 mg dried leaf powder in 10 ml distilled water in various conical flasks by keeping for stirring at 60°C for 3 h. After the aqueous solution with phytoconstituents were filtered and for them, the selected concentration, which was 10 ml of 4mM $AgNO_3$ solution was added then kept for the reaction at room temperature. From the above conditions, 40mg plant concentration and 4mM $AgNO_3$ have given good results, so for the optimize the pH condition five various pH solutions prepared at increasing pH gradually as 2, 4, 6, 8 and 10 which ascertained as the reaction proceeds instantly. The reaction time was examined by increasing the time for every 15 min, which was then monitored by recording the UV-Vis spectroscopy readings. After the optimization, nanosilver was bulkily prepared and accumulated through centrifugation.

Characterization of Synthesized Nanosilver: The establishment of nanosilver by way of reduction of Ag^+ ions was monitored by using measuring the UV-Vis spectroscopy (UV-Vis) in a wavelength range from 200-800 nm of the reaction mixture after diluting the small quantity of the sample with distilled water. The UV-Vis spectral analysis was implemented by using the instrument UV 2600 UV-Vis Spectrophotometer, Shimadzu. The Fourier Transform Infrared Spectroscopy (FTIR) analysis executed using KBr pellet devised from 1 mg of synthesized nanosilver was ground by blending with the small amount of potassium bromide, then the spectra had been recorded by using IR Affinity-1 Shimadzu model instrument, with 4500-500 cm^{-1} wavelength range.

The X-ray diffraction (XRD) analysis of nanosilver was evaluated with the aid of using Philips Xpert PRO, Instrument with Cukα X-ray source with generator settings 40kV, 30mAh with the scanning rate 2° min^{-1} in θ=2θ configuration. The Scanning Electron Microscopy - Energy Dispersive Spectroscopy (SEM-EDS) images as well as elemental analysis of the *Corchorus hirsutus* mediated nanosilver has been carried out by using model ZEISS Special Edition 18. A thin film of the sample was developed by dropping a small amount of the sample on the carbon coated copper grid; then the grid was permitted to dry for 10 min finally the pictures had been taken. Energy dispersive spectroscopy microanalysis system which automatically distinguishes the elements corresponded to the peaks in the energy distribution. For atomic force microscopy (AFM) analysis, the sample was dispersed in distilled water, followed by sonicated at 50 °C for 30 min. Then, a small, skinny film of the colloidal solution developed on a glass slide and permitted to dry, lately examined under model park systems XE7 atomic force microscopy.

Antibacterial Activity: The antibacterial property of synthesized nanosilver was investigated by the well-diffusion method. The sterilized nutrient agar medium was used to subculture the microorganism. The fresh cultures of antibacterial assays were prepared for four bacteria *Klebsiella pneumoniae*, *Bacillus subtillis, Staphylococcus aureus,* and *Pseudomonas putida*; all sterilized labware was utilized to execute this test.

The sterilized media were poured into the Petri plates at the laminar flow after solidification spread with 50 µl specific bacteria in each of the plates. The wells are perforated at 4 different places in the Petri plates and labeled then accordingly respective samples were added, in the end, Petri plates were incubated at 37 °C for 12 h to watch over the growth of bacteria.

Anticancer Activity:

Maintenance of Cell Line: The MCF7 breast cancer adenocarcinoma cell lines were purchased from NCCS, Pune and the cells were maintained in MEM supplemented with 10% FBS and the antibiotics penicillin/streptomycin (0.5 mL^{-1}), in an atmosphere of 5% CO_2/95% air at 37°C.

Preparation of Test Compound: For MTT assay, each test compounds were weighed separately and dissolved in DMSO. With media make up the final concentration of 1 mg/mL, and the cells were treated with a series of concentrations of 5-100 µg/mL. The cell viability was assessed by the MTT assay with three independent experiments with six concentrations of compounds in triplicates. MCF7 cells were trypsinized and execute the tryphan blue assay to know viable cells in the cell suspension. The cells were counted by hemocytometer and seeded at a density of 5.0×10^3 cells/well in 100 µl media in 96 well plate culture medium and incubated overnight at 37 °C. After incubation, take off the old media and add fresh media 100 µl with different concentrations of test compounds in representative wells in 96 plates.

After 48 h, discard the drug solution and the fresh medic with an MTT solution (0.5 $mg/mL^{-1)}$ were added to each well then the plates were incubated at 37°C for 3 h. At the end of incubation time, the precipitates are formed as a result of the reduction of the MTT salt to chromophore formazan crystals by the cells with metabolically active mitochondria. The optical density of solubilized crystals in DMSO was measured at 570 nm on a microplate reader. The percentage growth inhibition was calculated using the below-mentioned formula and concentration of test drug needed to inhibit cell growth by 50 % values is generated from the dose-response curves for each cell line using with origin software.

% of Inhibition = 100 (Control – Treatment / Control)

RESULTS AND DISCUSSION:

UV-Vis Spectroscopy: Optimized synthesis of nanosilver was monitored by noticing changes in the reaction mixture color and UV-Vis spectroscopy, which is an extensively used approach in the case of nanoparticles as they unveil surface plasmon phenomena (SPR) [18, 19]. The establishment of nanosilver particles was observed *via* this technique as the ionic silver becomes converted into stable metallic nanosilver. In all the cases of UV-Vis readings, the distinct absorption peaks were taken as an optimized condition which implies particles with nanosize with highly dispersed because of the broader peaks suggesting the larger particle sizes.

The uttermost absorption peaks were observed at 400-450 nm range, indicating the establishment of colloidal nanosilver. A single SPR peak unveils the isotropic, spherical shape nanoparticles in all the cases presented in **Fig. 2**, whereas multiple peaks are indicating the anisotropic particles [20]. In optimization initially, the reaction mixture exposes light reddish brown to dark brown at the very last levels was reasserting the formation of nanosilver particles. When increased the concentration of $AgNO_3$ as 1mM, 2mM, 3mM, the reaction given no peaks, where 4mM, 5Mm were given distinct characteristic peaks noticed in **Fig. 2a** which displays darkish brown color. When increasing the concentration of plant material pictured in **Fig. 2b** as 10 mg, 20 mg, 30 mg, 40 mg and 50 mg the reaction proceeds faster consequently more intense color and peaks were observed due to involving the more phytochemicals in the reaction [21, 22].

When the pH of the reaction mixture increases as pH 2, 4, 6, 8, 10, the more excessive brown color subsequently intense peaks were noticed which was depicted in **Fig. 2c.** The diverging color shades were observed from pH 6-10 while no color was observed at lower pH 2, 4 it indicates that the phytochemicals were likely to be inactivated at lower pH.

At the higher pH 8, 10 the reaction proceeds quicker in seconds, consequently conduces intense dark brown color. When increased the reaction time, the establishment of silver nanoparticles was increased, so the intensity of the peaks was elevated, as shown in **Fig. 2d**.

From all the above optimization studies 4 Mm $AgNO_3$ concentration, 40 mg plant concentration, pH 8, and 30 minutes reaction time have rendered distinct absorption peak at 412 nm so; it was selected for the bulk preparation of nanosilver.

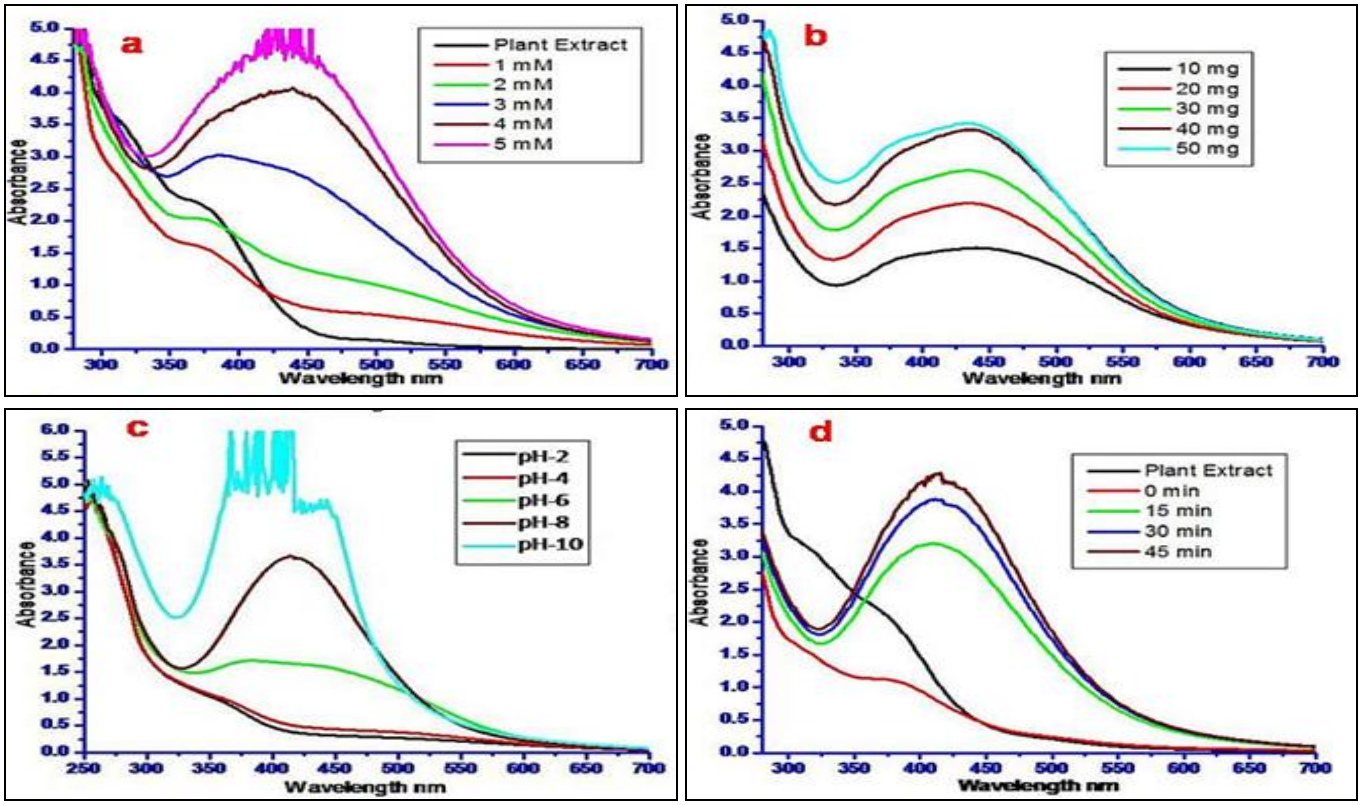

FIG. 2: UV-VIS SPECTROSCOPY OF (a) EFFECT OF $AgNO_3$ CONCENTRATION (b) EFFECT OF PLANT EXTRACT CONCENTRATION WITH SELECTED CONCENTRATION 4 mM $AgNO_3$ (c) EFFECT OF pH OF THE REACTION MIXTURE WITH SELECTED CONDITIONS 4 mM $AgNO_3$, 40 mg PLANT CONCENTRATIONS, (d) EFFECT OF REACTION TIME WITH SELECTED CONDITIONS 4 mM $AgNO_3$, 40 mg PLANT CONCENTRATIONS AND pH 8

FTIR Analysis: The principal objective to carry out the FTIR analysis was to oversee the functional groups of plant leaf extract as they were responsible for the reduction as well as stabilization of the nanosilver particles. The intense bands observed in **Fig. 3A** for silver at 3448, 2927, 2854, 1754, 1642, 1473, 1048 cm^{-1} and for the aqueous leaf extract 3438, 2927, 2854, 1642, 1464, 1058 cm^{-1}. The broadband observed at 3448 cm^{-1} suggests the strong stretching vibration of a hydroxyl group (-OH) from a phenolic compound.

The small sharp band at 2927, 2854 cm^{-1} correspond to the stretching vibrations of the O-H and C=O of aromatic and carbonyl groups of proteins, metabolites. The peak at 1754 cm^{-1} was ascribable C-O, C=O of aldehydes, carboxylic groups [23, 24], the peak at 1642 cm^{-1} credited to characteristic asymmetrical stretching with the carboxylate group. The symmetrical stretch of the carboxylate group attributed to the band in 1473 cm^{-1}. The peak at 1048 was credited to the alcoholic groups of C-O stretching. The FTIR spectrum of synthesized nanosilver reasserting the oxidation of above useful functional groups coupled with Ag ions in reduction.

X-ray Diffraction Studies: The X-ray diffraction studies are useful for the deciphering the crystalline nature of nanosilver. The **Fig. 3B** of XRD unveiling the Bragg's reflections with 2θ degrees of recordings as 38.06, 44.28, 64.49, 77.26 were comparable to the (111) (200) (220) (311) sets of lattice planes of nanosilver particles respectively. These recordings are strongly evoked the established nanoparticles were crystalline nature and also in a phase centric cubic structure[25] which is the good accord with the reference data of the joint action committee for powder diffraction studies (JCPDS 087-0720). The average particle size calculated from the below referred Debye-Scherrer equation[26] as it ranged from 13-69 nm.

A few unassigned peaks denoted by (*) also point out between characteristic peaks are perhaps ascribable the presence of phytochemicals environed to stabilize the nanoparticles [27].

$$D = K\lambda / \beta \cos\theta \text{ and } \beta = \pi / 180 \times FWHM$$

Where, *K* is the Scherrer constant with a value from 0.9 to 1 (shape factor), λ is the X-ray Wavelength (1.5418 Å), θ is the Bragg angle, the FWHM is full width at half maximum.

Scanning Electron Microscopy-Energy Dispersive Spectroscopy: Nearly spherical shaped particles had been depicted in **Fig. 4a** of SEM images. The images are showing the nano-size particles which were slightly aggregated; as a result, the larger particles had been generated. The presence of elemental silver was affirmed by using EDS spectral analysis [28, 29]. The principal signal was noted at ~3 KeV within the spectra of **Fig. 4b** indicates the presence of nanosilver [30, 31]; it is distinctive for the crystalline nature of synthesized nanosilver. The EDS spectrum unveils the strong signals for metallic Ag as it confirms the elemental components as an Ag weight % was 86.84, atomic % was 68.45 the same became offered in the EDS image of **Fig. 4c**. Other signals are also recorded were due to elements of phytochemicals from leaf extract.

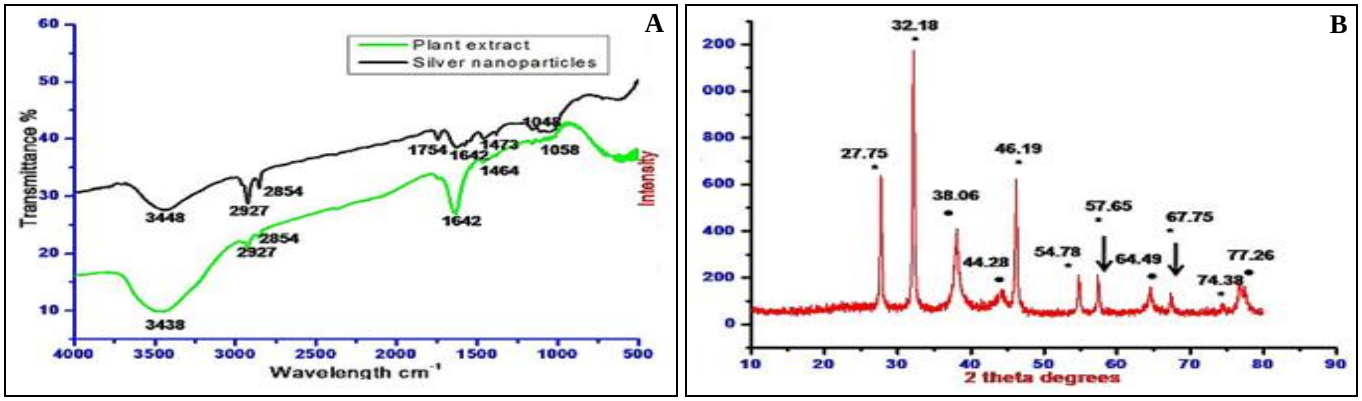

FIG. 3: (A) FTIR SPECTRA OF THE VARIOUS BANDS FOR THE *CORCHORUS HIRSUTUS* PLANT EXTRACT AND SYNTHESIZED NANOSILVER, (B) XRD OF THE MAIN PEAKS FOUND IN SPECTRA REVEALING THE CRYSTALLINE STRUCTURE OF THE *CORCHORUS HIRSUTUS* MEDIATED NANOSILVER

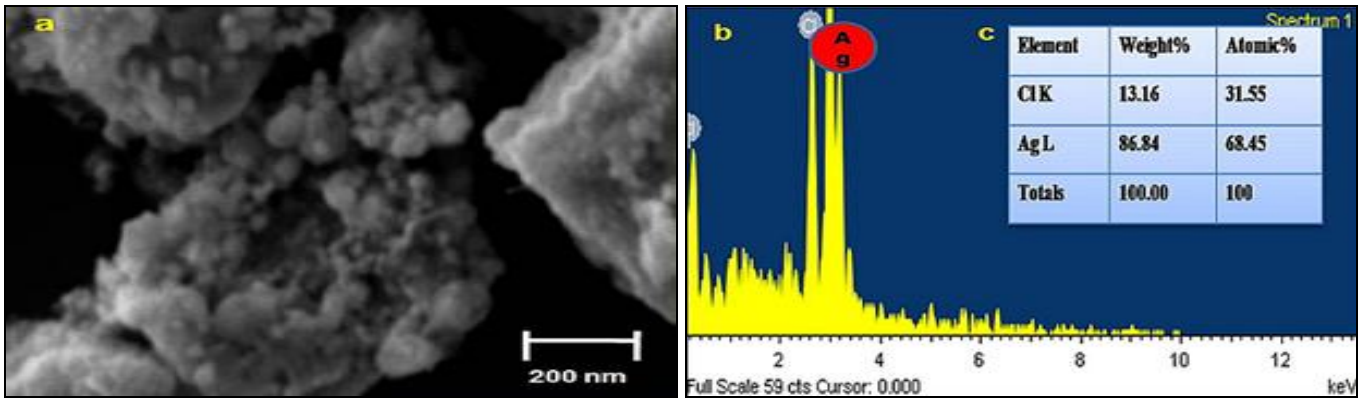

FIG. 4: (A) SEM IMAGES OF *CORCHORUS HIRSUTUS* MEDIATED NANOSILVER (B) EDS SPECTRA OF ELEMENTAL SIGNALS OF Ag (C) THE ATOMIC %, AND WEIGHT % OF *CORCHORUS HIRSUTUS* MEDIATED NANOSILVER

Atomic Force Microscope: The AFM is a widely used approach for inspecting the dimensions of the nanoparticles. The topographical structure of the established nanosilver particles was depicted in **Fig. 5** by AFM. The 3D images in **Fig. 5a** of particles on the surface of the sample. The 3D images offer the information about roughness and clusters forming by aggregation in addition to this; single particles were also observed as a result of sonication before the examination and evidencing the nanoparticles were in below 50 nm in height. The 2D image of **Fig. 5b** horizontal cross section of red line shows the spherically shaped particles below 10 nm size.

Antibacterial Activity: Now a day's microbes are turning more potent to many antibiotics, for this reason, there has been essential in the manufacturing of novel drugs as nanosilver having antifungal, antibacterial [32] and antiviral [33] properties in opposition to pathogens. The well - known inhibitory effect of silver has been acknowledged for several years back and continuously using for various medical applications.

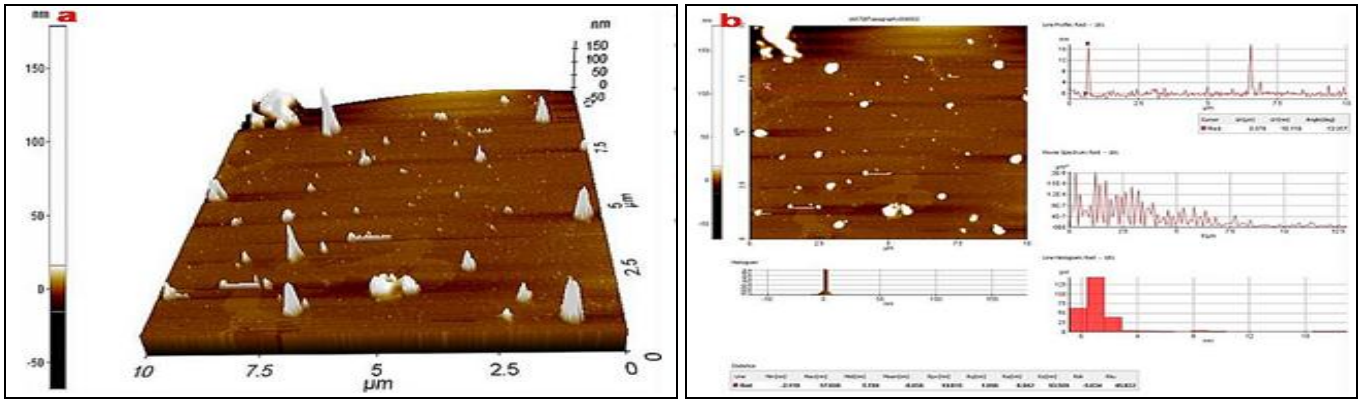

FIG. 5: AFM IMAGES OF NANOSILVER (A) THE 3D IMAGE (B) 2D IMAGE OF SMALL SIZED, SPHERICAL SHAPED PARTICLES

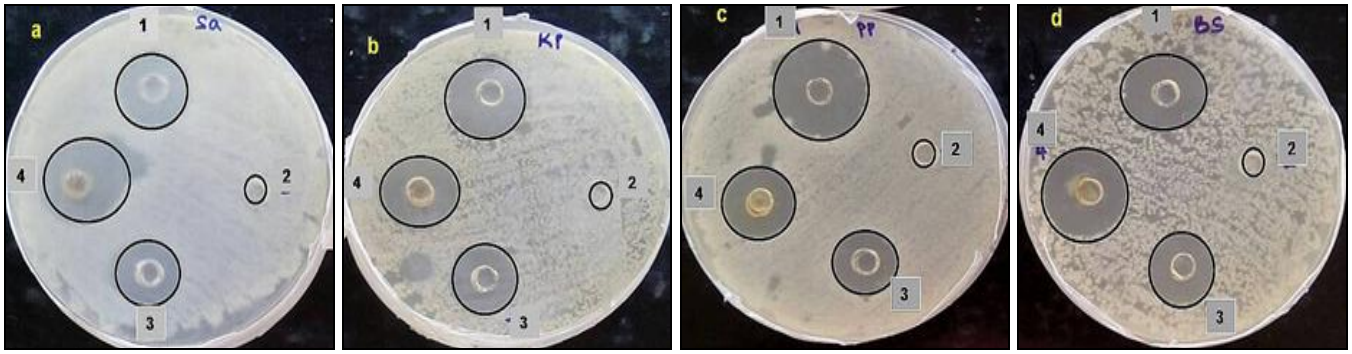

FIG. 6: ANTIBACTERIAL PROPERTY ILLUSTRATES THE ZONE OF INHIBITION FOR DIFFERENT BACTERIA (A) *STAPHYLOCOCCUS AUREUS* (B) *KLEBSIELLA PNEUMONIA* (C) *PSEUDOMONAS PUTIDA* (D) *BACILLUS SUBTILIS* FOR THE SAMPLES, INDICATING, 1-AMPICILLIN 2-PLANT EXTRACT, 3-$AgNO_3$, AND 4-NANOSILVER PARTICLES IN EACH PLATE

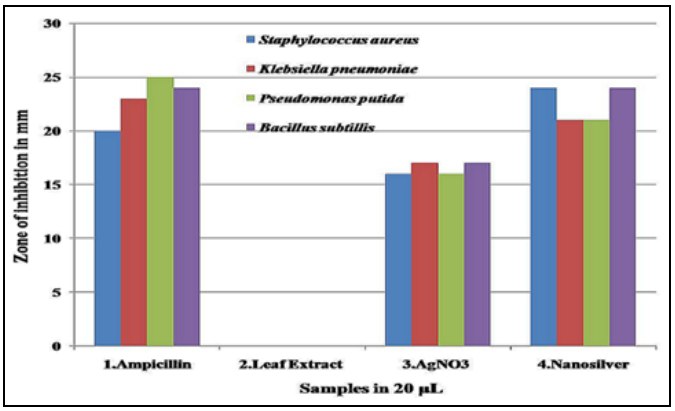

FIG. 7: BAR GRAPH OF ZONE OF INHIBITION OF THE BACTERIA ALONG WITH SAMPLES USED IN ANTIBACTERIAL TEST

To examine the antibacterial activity of the nanosilver established by using *Corchorus hirsutus* leaf extract, the well-diffusion method was employed, as shown in **Fig. 6**. The efficient antibacterial activity of nanosilver ascertained by the zone of inhibition found in opposition to four tested strains *Staphylococcus aureus, Klebsiella pneumoniae*, *Pseudomonas putida*, and *Bacillus subtilis* as 24 mm, 21 mm, 21 mm and 24 mm respectively as expressed in **Fig. 7** of the bar graph along with the other tested samples. Synthesized nanosilver exhibited good antibacterial activity when compared to the $AgNO_3$ for all four tested bacteria. The aqueous leaf of *Corchorus hirsutus* doesn't show any activity against four bacteria as it may be due to the very low concentration used. The highest activity was observed more than controlled drugs in the case of *Staphylococcus aureus.* The precise mechanism of silver nanoparticles engages to induce an antimicrobial effect is not explicitly recognized. The study of the antibacterial effect of nanosilver particles on microorganisms concluded

that the highest conductivity of cells treated with nanosilver might be due to the silver nanoparticles hoarded on the surface of bacteria by attaching to cell wall of bacteria, then cause penetration which directs breakage of cell wall subsequently leads to cell death [34], or due to the release of the cellular components present inside the cells by binding to the phosphorous and nitrogen groups of DNA in the cells eventually causes to breakage to strands and leads to cell death [35]. The outstanding antibacterial effect in the current study perhaps provides a new standard in the field of development of new antibacterial agents.

Anticancer Activity: The cytotoxic activity of *Corchorus hirsutus* mediated nanosilver was examined by using MTT assay against MCF-7 [36], HeLa cell lines [37, 38] at various concentrations. The morphological changes were displayed in **Fig. 8**. The cancer cell membrane lysis was observed by increasing the concentration of the nanosilver. The images exhibiting the apoptosis dependent pathway as the apoptosis rate was more in a higher concentration of nanosilver by the nanosilver interacted with the functioning of proteins in cancer cells then pushes to cell lysis.

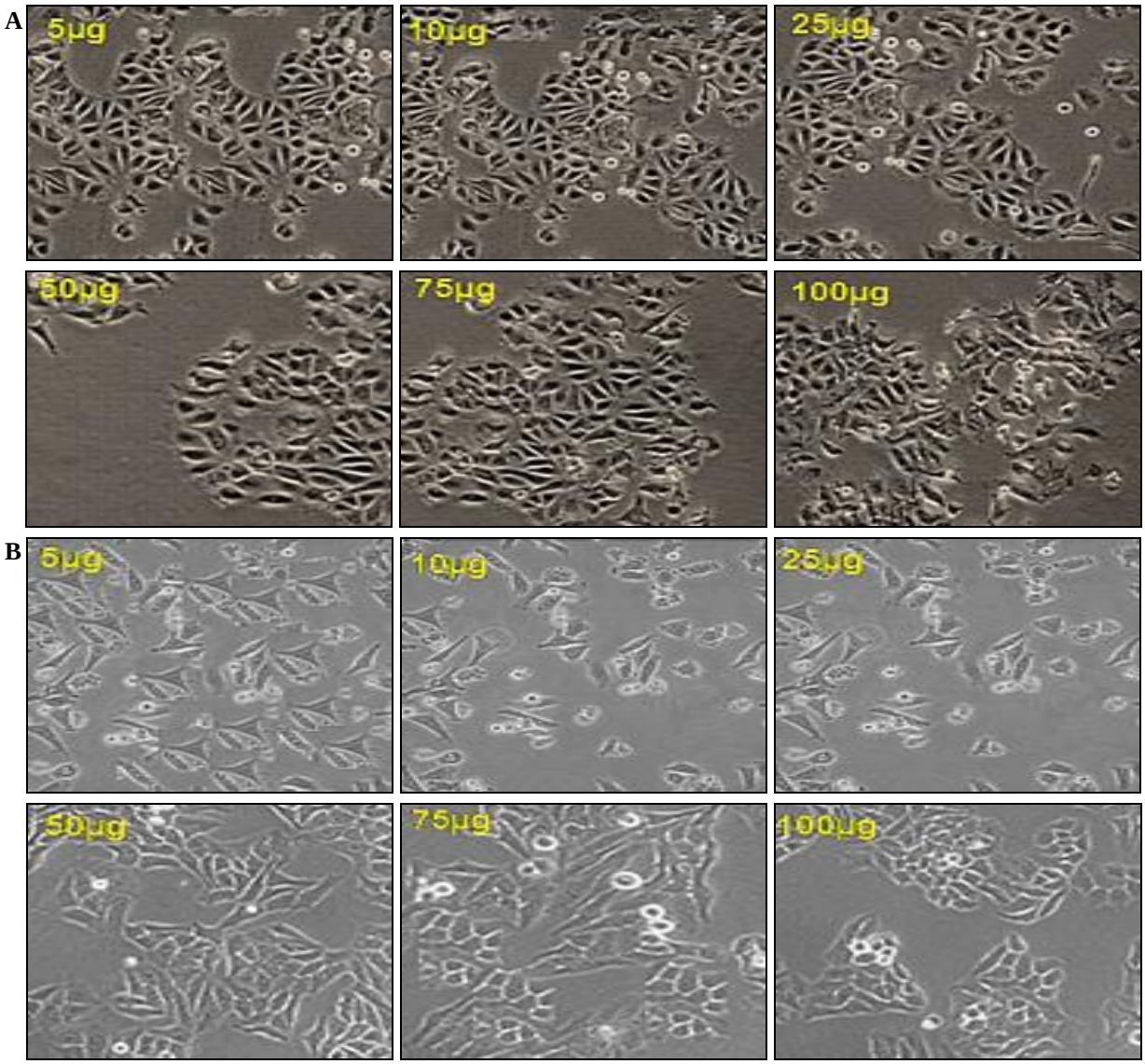

FIG. 8: CYTOTOXIC EFFECT ON (A) MCF7 CELL LINE (B) HeLa CELL LINE AFTER TREATMENT OF NANOSILVER SHOWED CHANGES IN THE CELL MORPHOLOGY

The above analyses are exposing that these *Corchorus hirsutus* mediated nanosilver exerts the outstanding cytotoxic effect on MCF7 cell lines of breast cancer adenocarcinoma cells and HeLa cell lines of cervical cancer cells. The IC_{50} values, % of viability with tested different nanosilver concentrations, were presented in **Table 1** for two cell lines. The IC_{50} values found to be 37.66 µg/mL

for MCF7 cell lines, 43.69 µg/mL for HeLa cell lines. The IC_{50} values worked out through the graph shown in **Fig. 9,** which was plotted as concentration (µg/mL) against the % of viability.

TABLE 1: CYTOTOXIC PROPERTIES OF NANOSILVER ON MCF7 AND HeLa CELL LINES

Concentration (µg/mL)	Average		Average-Blank		% Viability		IC_{50} (µg/mL)	
	MCF7	HeLa	MCF7	HeLa	MCF7	HeLa	MCF 7	HeLa
100	0.317	0.443	0.312	0.44	14.885	21.103	37.66	43.69
75	0.643	0.903	0.638	0.9	30.438	43.165		
50	0.959	1.137	0.954	1.134	45.515	54.388		
25	1.117	1.201	1.112	1.198	53.053	57.458		
10	1.384	1.232	1.379	1.229	65.792	58.944		
5	1.45	1.334	1.445	1.331	68.94	63.836		
Untreated	2.101	2.088	2.096	2.085	100	100		
Blank	0.005	0.003	0	0	0	0		

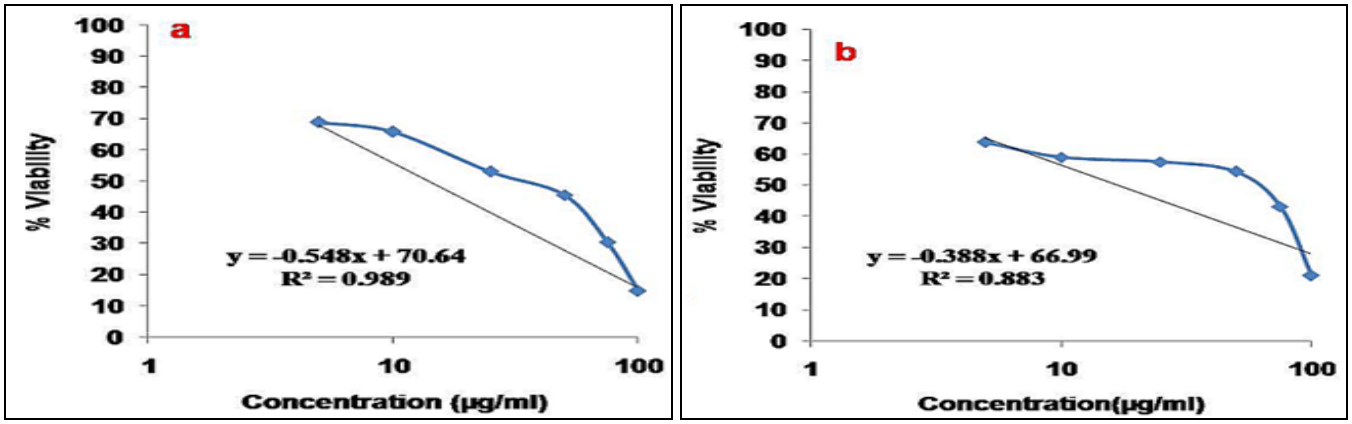

FIG. 9: LINE GRAPH OF CYTOTOXIC EFFECT OF THE NANOSILVER ON (A) MCF7 CELL LINE (B) HeLa CELL LINE

Measurement of cell viability and proliferation forms the basis for numerous *in-vitro* assays of a cell population's response to external factors. The MTT cell proliferation assay measures the cell proliferation rate and conversely, when metabolic events leading to apoptosis or necrosis, the reduction in cell viability. MTT Assay is a colorimetric assay that measures the reduction of yellow 3-(4, 5-dimethythiazol- 2-yl)-2, 5-diphenyl tetrazolium bromide (MTT) by mitochondrial succinate dehydrogenase. The assay depends both on the number of cells present and on the assumption that dead cells or their products do not reduce tetrazolium. The MTT enters the cells then passes into the mitochondria where it is reduced to an insoluble, dark purple colored formazan crystals. The cells are then solubilized with a DMSO and released; solubilized formazan reagent is measured spectrophotometrically at 570 nm.

CONCLUSION: Optimized synthesis of nano-silver particles became achieved efficaciously from silver nitrate as a precursor and *Corchorus hirsutus* aqueous leaf extract reducing as well as a stabilizing agent for the first time from the phytosynthesized method. The optimization produces efficient synthesis by way of controlling the size and shape of the particles of interest. The performed biological method was cost-effective, eco-friendly technique, simple process and compatibility for biomedical and pharmaceutical diligent efforts for the larger scale commercial production.

The characterization of synthesized nanosilver furnishes information about its reduction with phytochemicals, crystalline nature, spherical shape and average size, which found to be 29 nm. The synthesized nanoparticles show the profound effect against human pathogens tested and cytotoxic activity investigated against MCF7 cell lines of breast cancer adenocarcinoma cells and HeLa cell lines of cervical cancer cells, suggesting that these *Corchorus hirsutus* mediated nanosilver can be used as antibacterial and anticancer agents as they may provide a promising effective drug in a chemotherapeutic remedy.

ACKNOWLEDGEMENT: The authors gratefully acknowledge the Forensic Science Unit, Department of Chemistry for providing facilities to carry out the research. One of the authors SR thankful to University grants commission, New Delhi, India for awarding Senior Research Fellowship.

CONFLICT OF INTEREST: The authors declare that they have no conflict of interest.

REFERENCES:

1. Kreuter J: Peroral administration of nanoparticles. Advanced Drug Delivery Reviews 1991; 7(1): 71-86.
2. Pandian N and Chidambaram S: Antimicrobial, cytotoxicity and anticancer activity of silver nanoparticles from *Glycyrrhiza glabra*. Int J Pharm Sci Res 2015; 41: 1633-1641.
3. Cantu Antonio A: Optics and Photonics for Counterterrorism and Crime Fighting IV. The United Kingdom, SPIE Proceedings Vol. 7119, 2008: 71190F.
4. Li H, Li F, Wang L, Sheng J, Xin Z, Zhao L, Xiao H, Zheng Y and Hu Q: Effect of nano-packing on preservation quality of Chinese jujube *(Ziziphus jujuba* Mill. var. inermis (Bunge Rehd). Food Chemistry 2008; 114 (2): 547-52.
5. Park HJ, Sung HK, Kim HJ and Choi SH: A new composition of nanosized silica-silver for control of various plant diseases. Plant Pathol J 2006; 22: 295-302.
6. Buzea C, Pacheco II and Robbie K: Nanomaterials and nanoparticles, sources and toxicity. Biointerphases 2007; 2(4): MR17-MR71.
7. Singh J, Singh N, Rathi A, Kukkar D and Rawat M: Facile approach to synthesize and characterization of silver nanoparticles by using mulberry leaves extract in aqueous medium and its application in antimicrobial activity. J Nanostructures 2017; 7(2): 134-40.
8. Rao B and Ren-Cheng T: Green synthesis of silver nanoparticles with antibacterial activities using aqueous *Eriobotrya japonica* leaf extract. Adv Nat Sci Nanosci Nanotechnol 2017; 8(1): 1-8.
9. Nagajyothi PC, Sreekanth TVM, Lee JI and Lee KD: Mycosynthesis: antibacterial, antioxidant and anti-proliferative activities of silver nanoparticles synthesized from *Inonotus obliquus* (Chaga mushroom) extract. J Photochem Photobiol B Biol 2014; 130: 299-04.
10. Tippayawat P, Phromviyo N, Boueroy P and Chompoosor A: Green synthesis of silver nanoparticles in *Aloe vera* plant extract prepared by a hydrothermal method and their synergistic antibacterial activity. Peer J 2016; 4: e2589.
11. Lokina S, Stephen A, Kaviyarasan V, Arulvasu C and Narayanan V: Cytotoxicity and antimicrobial activities of green synthesized silver nanoparticles. Eur J Med Chem 2014; 76: 256-63.
12. Ahmed S, Ahmad M, Swami BL and Ikram S: Green synthesis of silver nanoparticles using *Azadirachta indica* aqueous leaf extract. J Radiat Res Apl Sci 2016; 9(1): 1-7.
13. Dubey SP, Lahtinen M and Sillanpa M: Green synthesis and characterization of silver and gold nanoparticles using leaf extract of *Rosa rugosa*. Colloid Surf A Physicochem Eng Aspect 2010; 364: 34–41.
14. Geethalakshmi E and Sarada DV: Synthesis of plant-mediated silver nanoparticles using *Trianthema decandra* extract and evaluation of their antimicrobial activities. Int J Eng Sci Tech 2010; 2: 970-75.
15. Vadlapudi V and Kaladhar DSVGK: Review: green synthesis of silver and gold nanoparticles. Middle-East Journal of Scientific Research 2014; 19(6): 834-42.
16. Mahdi S, Taghdiri M, Makari V and Rahimi-Nasrabadi M: Procedure optimization for green synthesis of silver nanoparticles by aqueous extract of *Eucalyptus oleosa*. Spectrochimica Acta Part A: Molecular and Biomolecular Spectroscopy 2015; 136: 1249-54.
17. Rai A, Singh A, Ahmad A and Sastry M: Role of halide ions and temperature on the morphology of biologically synthesized gold nanotriangles. Langmuir 2006; 22(2): 736-41.
18. Mulvaney P: Surface plasmon spectroscopy of nanosized metal particles. Langmuir 1996; 12: 788-00.
19. Krishnaraj C, Jagan EG, Rajasekar S, Selvakumar P, Kalaichelvan PT and Mohan N: Synthesis of silver nanoparticles using *Acalypha indica* leaf extracts and its antimicrobial activity against water borne pathogens. Colloids Surf B Biointerfaces 2010; 76: 50-56.
20. Satishkumar M, Sneha K, Won SW, Cho CW, Kim S and Yun YS: *Cinnamon zeylanicum* bark extract and powder mediated green synthesis of nano-crystalline silver particles and its antibacterial activity. Colloids and Surfaces, B: Biointerfaces 2009; 73: 332-38.
21. Huang J, Li Q, Sun D, Lu Y, Su Y, Yang X, Wang H, Wang Y, Shao W, He N, Hong J and Chen C: Biosynthesis of silver and gold nanoparticles by novel sundried *Cinnamomum camphora* leaf. Nanotechnology 2007; 18: 105104-14.
22. Philip D: Biosynthesis of Au, Ag and Au-Ag nanoparticles using edible mushroom extract. Spectrochim Acta. A Mol Biomol Spectrosc 2009; 73(2): 374-81.
23. Shankar SS, Ahmad A and Sastry M: Geranium leaf assisted biosynthesis of silver nanoparticles. Biotechnol Prog 2003; 19: 1627-31.
24. Shameli K, Ahmad M.B, Yunus WMZW and Ibrahim NA: Synthesis and characterization of silver/talc nano-composites using the wet chemical reduction method. Int J. Nanomed 2010; 5: 743-51.
25. Vidhu VK, Aromal A and Philip D: Green synthesis of silver nanoparticles using *Macrotyloma uniflorum*. Spectrochim Acta A Mol Biomol Spectros 2011; 83: 392-97.
26. Satyavathi R, Krishna MB, Rao SV, Saritha R and Rao DN: Biosynthesis of silver nanoparticles using *Coriandrum sativum* leaf extract and their application in nonlinear optics. Adv Sci Lett 2010; 3: 1-6.
27. Prasad KS, Pathak D, Patel A, Dalwadi P, Prasad R, Patel P and Selvaraj K: Biogenic synthesis of silver nanoparticles using *Nicotiana tobaccum* leaf extract and study of their antibacterial effect. African Journal of Biotechnology 2011; 10(41): 8122-30.
28. Saxena A, Tripathi RM and Singh RP: Biological synthesis of silver nanoparticles by using onion (*Allium cepa*) extract and their antibacterial activity. Digest Journal of Nanomaterials and Biostructures 2010; 5(2): 427-32.
29. Kaviya S, Santhanalakshmi J, Viswanathan B, Muthumary J and Srinivasan K: Biosynthesis of silver nanoparticles using *Citrus sinensis* peel extract and its antibacterial activity. Spectrochim Acta A 2011; 79: 594-98.
30. Kanipandian N, Kannan S, Ramesh R, Subramanian P and Thirumurugan R: Characterization, antioxidant and cytotoxicity evaluation of green synthesized silver nanoparticles using *Cleistanthus collinus* extract as a surface modifier. Mater Res Bull 2014; 49: 494-02.

31. Panacek A, Kolar M, Vecerova R, Prucek R, Soukupova J, Krystof V, Hamal P, Zboril R and Kvitek L: Antifungal activity of silver nanoparticles against *Candida spp*. Biometals 2009; 30: 6333-40.
32. Lara HH, Ayala-Nuñez NV, Ixtepan-Turrent L and Rodriguez-Padilla C: Mode of antiviral action of silver nanoparticles against HIV-1. J Nanobiotechnology 2010; 8: 1-10.
33. Hidalgo E and Dominguez C: Study of cytotoxicity mechanisms of silver nitrate in human dermal fibroblasts. J. Toxicol Lett 1998; 98: 169-79.
34. Sondi I and Salopek-Sondi B: Silver nanoparticles as antimicrobial agent: a case study on *E. coli* as a model for Gram-negative bacteria. J Colloid Interface Sci 2004; 275: 177-82.
35. Vivek R, Thangam R, Muthuchelian K, Gunasekaran P, Kaveri K and Kannan S: Green biosynthesis of silver nanoparticles from *Annona squamosa* leaf extract and its *in-vitro* cytotoxic effect on MCF7 cells. Process Biochemistry 2012; 47(12): 2405-10.
36. Heydari R and Marzieh R: Green synthesis of silver nanoparticles using the extract of oak fruit hull (Jaft): synthesis and *in-vitro* cytotoxic effect on MCF7 Cells. International J of Breast Cancer 2015; 47(2): 273-79.
37. Sukirtha R, Priyanka KM, Antony JJ, Soundararajan K, Ramar T, Gunasekaran P, Krishnan M and Achiraman S: Cytotoxic effect of green synthesized silver nanoparticles using *Melia azedarach* against *in-vitro* HeLa cell lines and lymphoma mice model. Pro Bioche 2012; 47(2): 273-79.
38. Miura N and Shinohara Y: Cytotoxic effect and apoptosis induction by silver nanoparticles in HeLa cells. Biochemical and Biophysical Research Communications 2009; 390(3): 733-37.

How to cite this article:
Ashok D, Raju S and Rama K: Assessment of *in-vitro* anticancer and antibacterial activities of *Carchorus hirsutus* phytomediated optimized nanosilver. Int J Pharm Sci & Res 2019; 10(10): 4587-97. doi: 10.13040/IJPSR.0975-8232.10(10).4587-97.